Cell

HIV Enters Cells via Endocytosis and Dynamin-Dependent Fusion with Endosomes

Kosuke Miyauchi,[1,2] Yuri Kim,[1,2] Olga Latinovic,[1] Vladimir Morozov,[1] and Gregory B. Melikyan[1,*]
[1]Institute of Human Virology and Department of Microbiology and Immunology, University of Maryland School of Medicine, 725 W. Lombard Street, Baltimore, MD 21201, USA
[2]These authors contributed equally to this work
*Correspondence: gmelikian@ihv.umaryland.edu
DOI 10.1016/j.cell.2009.02.046

SUMMARY

Enveloped viruses that rely on a low pH-dependent step for entry initiate infection by fusing with acidic endosomes, whereas the entry sites for pH-independent viruses, such as HIV-1, have not been defined. These viruses have long been assumed to fuse directly with the plasma membrane. Here we used population-based measurements of the viral content delivery into the cytosol and time-resolved imaging of single viruses to demonstrate that complete HIV-1 fusion occurred in endosomes. In contrast, viral fusion with the plasma membrane did not progress beyond the lipid mixing step. HIV-1 underwent receptor-mediated internalization long before endosomal fusion, thus minimizing the surface exposure of conserved viral epitopes during fusion and reducing the efficacy of inhibitors targeting these epitopes. We also show that, strikingly, endosomal fusion is sensitive to a dynamin inhibitor, dynasore. These findings imply that HIV-1 infects cells via endocytosis and envelope glycoprotein- and dynamin-dependent fusion with intracellular compartments.

INTRODUCTION

Endocytosis is an obligatory entry step for enveloped viruses whose fusion proteins are activated by acidic pH (Marsh and Helenius, 2006). In contrast, viruses that undergo fusion upon interacting with cognate cellular receptors irrespective of the pH are thought to fuse directly with a plasma membrane. For instance, HIV-cell fusion initiated upon sequential interactions of the envelope (Env) glycoprotein with CD4 and coreceptors CCR5 or CXCR4 (e.g., Doms and Trono, 2000) has long been assumed to occur at the cell surface, whereas internalized virions were thought to be degraded by cells (Maddon et al., 1988; McClure et al., 1988; Pelchen-Matthews et al., 1995; Stein et al., 1987). This notion is supported by the fact that HIV can mediate fusion between adjacent target cells ("fusion from without") and that HIV Env expressed on effector cells promotes fusion with target cells at neutral pH. In addition, mutations in CD4 or coreceptors (CR) that impair their ligand-induced internalization do not block HIV-1 infection (Brandt et al., 2002; Maddon et al., 1988). The fact that pseudotyping the HIV core with the low pH-dependent G glycoprotein of Vesicular Stomatitis Virus (VSV) eliminates the Nef requirement for optimal infectivity (Aiken, 1997) is indicative of different entry routes for these and HIV Env-bearing viruses. In addition, the restriction on HIV-1 infection in resting T cells imposed by the cortical actin is consistent with fusion at the cell surface (Yoder et al., 2008).

On the other hand, several lines of evidence support the existence of an alternative endocytic pathway for HIV-1 entry. First, HIV fusion with endosomes and micropinosomes has been observed by electron microscopy (Marechal et al., 2001; Pauza and Price, 1988). Second, blocking the acidification of endosomal compartments can augment HIV infection, apparently by sparing the virus from degradation in lysosomes (Fredericksen et al., 2002; Schaeffer et al., 2004; Wei et al., 2005). Third, efficient infection by HIV particles pseudotyped with VSV G (Aiken, 1997) shows that there are no apparent restrictions associated with the endocytic entry pathway. Finally, inhibition of clathrin-mediated endocytosis reduces the efficacy of HIV-cell fusion and infection in HeLa-derived cells (Daecke et al., 2005). However, this intervention perturbs important cellular functions and may thus alter the sites of virus entry.

Here, we applied time-resolved single-virus imaging and a virus population-based fusion assay to delineate the cellular entry sites of HIV-1. These approaches have revealed that, surprisingly, complete HIV-1 fusion occurred in endosomal compartments but not at the plasma membrane of epithelial and lymphoid cells. We found that endosomal fusion was delayed relative to HIV-1 uptake via CD4/CR-dependent endocytosis and that the fusion step was enhanced by the large GTPase dynamin. Methodologies developed in this work should help define the entry pathways of other pH-independent viruses.

RESULTS

To elucidate the sites of virus entry, we first compared the effects of fusion inhibitors blocking surface-accessible viruses and universal inhibitors that block all viruses irrespective of their location. If fusion is limited to the cell surface, these interventions should yield identical results. However, the ability to enter into and fuse with endosomes would result in the transient appearance of viruses resistant to external inhibitors but sensitive to inhibitors blocking endosomal fusion. The difference in virus sensitivity to site-specific and universal inhibitors can thus be used to deduce the entry sites of pH-independent viruses.

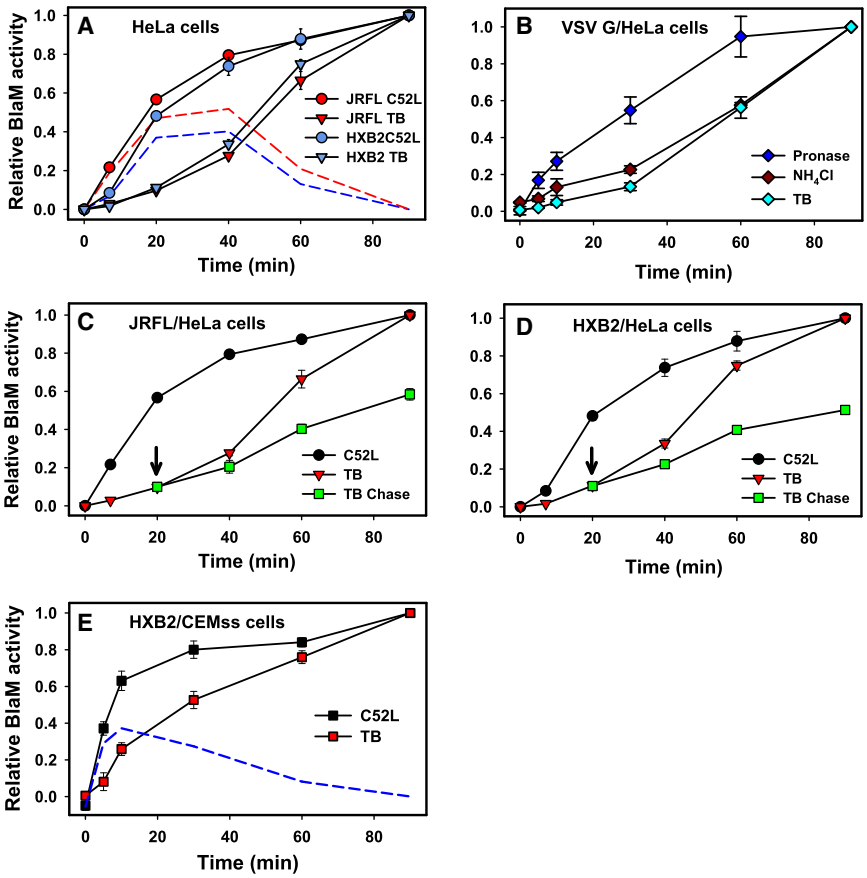

Figure 1. Dissection of Surface and Endosomal HIV-1 Fusion

(A) Virus fusion with TZM-bl cells was stopped by adding C52L after indicated times of incubation at 37°C, and incubation was continued up to 90 min, at which point the cells were briefly placed on ice and loaded with the BlaM substrate. Alternatively, fusion was stopped by placing cells on ice after varied times of incubation at 37°C (TB). After loading the substrate, cells were incubated overnight at 13.5°C regardless of the fusion protocol to allow the substrate cleavage. The red and blue dashed lines were obtained by subtracting the TB plot from the C52L escape plot for JRFL and HXB2, respectively. Unless stated otherwise, data points are means ± standard error of the mean (SEM) from triplicate measurements.

(B) Fusion of VSV G pseudotypes with TZM-bl cells was blocked at indicated times either by treating cells with 2 mg/ml pronase on ice (10 min), adding 50 mM NH_4Cl, or chilling the samples (TB). Cells were then loaded with CCF2 and incubated overnight at 12°C.

(C and D) After 20 min at 37°C, viruses remaining at the surface of TZM-bl cells were rendered nonfusogenic by adding C52L (arrow), and the extent of fusion over time at 37°C was determined by chilling cells either immediately or at indicated time points (green squares).

(E) HXB2 virus escape from C52L and from the TB in CEMss cells was measured as described above. The dashed blue line represents the difference between the C52L and TB curves. Error bars are SEM (n = 4).

HIV-1 Fusion Is Delayed Relative to Its Escape from a Membrane-Impermeant Fusion Inhibitor

Virus-cell fusion was directly quantified by measuring the cytosolic activity of viral core-associated β-lactamase (BlaM) (Cavrois et al., 2002). HIV-1 cores carrying a BlaM-Vpr chimera were pseudotyped with Env from JRFL (CCR5-tropic) or HXB2 (CXCR4-tropic) HIV-1 strains. We first examined the HIV-1 entry sites in HeLa-derived indicator cells expressing CD4, CCR5, and CXCR4 (designated TZM-bl cells; Wei et al., 2002). Viruses were allowed to bind to cells in the cold, and fusion was initiated by shifting to 37°C and measured as the extent of cleavage of a fluorogenic substrate by the cytosolic BlaM-Vpr. To determine the kinetics of virus-cell fusion, we stopped the reaction after varied times of incubation at 37°C by adding a recombinant peptide derived from the C-terminal heptad repeat region of HIV-1 gp41 (hereafter referred to as C52L; Deng et al., 2007). C52L and other gp41-derived peptides inhibit fusion by binding to intermediate gp41 conformations formed upon Env interactions with CD4 and CR and preventing the formation of the final 6-helix bundle structure (reviewed in Eckert and Kim, 2001). The time of C52L addition experiments revealed that the kinetics of the JRFL and HXB2 escape from this membrane-impermeant inhibitor was relatively fast, showing little or no lag and reaching completion within ~2 hr (Figure 1A).

To block HIV-1 fusion irrespective of its cellular location, we took advantage of the steep temperature dependence of HIV-1 fusion (Frey et al., 1995; Mkrtchyan et al., 2005). JRFL and HXB2 fusion with TZM-bl cells exhibited a well-defined threshold at ~22°C (Figure S1A available online). By contrast, the cytosolic BlaM was active at temperatures that were not permissive for fusion (data not shown). This allowed kinetic measurements of virus-cell fusion by quickly reducing the temperature after varied times of incubation at 37°C, followed by an overnight incubation at subthreshold temperature to permit substrate cleavage.

The temperature block (TB) protocol showed that, surprisingly, the cytosolic BlaM delivery was greatly delayed compared to the virus escape from C52L (Figure 1A). This delayed kinetics can result from two principal mechanisms. Low temperature can either block Env-mediated fusion or inhibit post-fusion steps that may be required for the optimal activity of the viral core-associated BlaM-Vpr. However, previous work (Cavrois et al., 2004) and our data (Figure S1B) show that the post-fusion uncoating step does not enhance the BlaM activity. We found that this activity was not affected by inhibition of cellular proteases or proteasomes and, importantly, was observed in vitro in the absence of any cytosolic factors (Figures S1C–S1E). Thus, the cleavage of BlaM substrate faithfully reports the extent of virus-cell fusion.

Our experimental strategy to elucidate the sites of virus entry was further validated using HIV particles pseudotyped with the low pH-dependent VSV G. As expected for an endocytic entry pathway, escape from the TB was delayed relative to the virus uptake measured by the emergence of the BlaM signal resistant to pronase (Figure 1B). The temperature-dependent steps of

VSV G fusion were completed soon after the completion of low pH-dependent steps, as measured by the virus, escape from the block imposed by NH_4Cl. The quick appearance of the TB-resistant BlaM signal after the low pH-induced fusion further implies that temperature-dependent post-fusion steps are not required to render BlaM-Vpr active.

HIV-1 Likely Enters Lymphoid Cells through an Endocytic Pathway

To define the sites of HIV entry in more natural target cells, we measured the rates of virus escape from C52L and from the TB in lymphoid CEMss cells expressing CD4 and CXCR4. In these cells, both rates were considerably faster than in TZM-bl cells (Figure 1E versus Figure 1A). However, the loss of sensitivity to C52L occurred much earlier than the progression beyond temperature-dependent steps, suggesting that endosomal fusion is the major HIV-1 entry route in T cells.

HIV-1 Associated with CD4 and Coreceptors Spends Considerable Time in Endosomes prior to Fusion

The divergent rates of HIV-1 escape from C52L and the TB demonstrate that the actual fusion is much slower than the loss of sensitivity to the membrane-impermeant fusion inhibitor, which has been customarily interpreted as fusion with the plasma membrane. The difference between the C52L- and TB-resistant BlaM signals should reflect the fraction of internalized viruses that have not fused at that time point (Figure 1A, dashed lines). Within the first 20 min of incubation, ~40% of viruses appeared in C52L-inaccessible compartments, while only a small fraction acquired resistance to the TB. The high level of internalized viruses was maintained during the next 20 min due to the similar rates of escape from C52L (endocytosis) and the TB (fusion). Likewise, nearly half of the viruses were protected from C52L but did not fuse with CEMss cells within the first 10 min at 37°C (Figure 1E, dashed line). Collectively, these findings show that HIV-1 fuses primarily, if not exclusively, with endosomes.

In order to separate plasma membrane entry from endosomal entry, viruses were prebound to cells in the cold and incubated at 37°C for 20 min, at which point surface-accessible unfused viruses were blocked by C52L. The BlaM signal was then chased by dropping the temperature either immediately or after varied times of incubation at 37°C in the presence of the inhibitor. Under these conditions, any increase in the BlaM signal over time should be exclusively due to viral content release from endosomes. The chase experiments revealed that endosomal fusion progressed slowly (Figures 1C and 1D), reaching completion within ~1 hr at 37°C. As expected, the regular TB protocol yielded much greater extents of fusion compared to the chase protocol (red triangles versus green squares), which was most likely due to the continued uptake and fusion of surface-accessible viruses in the absence of the inhibitor. Thus, on average, HIV-1 spent about 30 min in C52L-inaccessible compartments prior to releasing its content.

In the absence of surface fusion, protection from C52L should correspond to productive, CD4/CR-mediated HIV endocytosis. This notion is supported by the ability of C52L to block fusion when added at the beginning of incubation, demonstrating that the gp41 coiled coils are exposed prior to virus uptake; this exposure is known to occur upon Env binding to CD4 alone or to CD4 and CR (Eckert and Kim, 2001 and references therein). Accordingly, HIV-1 acquired resistance to inhibitors blocking CD4 and CR binding before it escaped from C52L (Figure S1F). Thus, HIV-1 particles internalized by pathways other than CD4/CR-mediated endocytosis do not contribute to fusion. These results and virus imaging data (see below) show that, surprisingly, the major rate-limiting step of HIV-1 fusion occurs after CR binding and virus endocytosis.

Single-Virus Imaging Distinguishes between Surface and Endosomal Fusion

To unambiguously identify the sites of HIV-1 entry, we visualized the fusion of viruses colabeled with the relatively small, diffusible content marker (NC-GFP, Figures S2B, S2D, and S2E) and the lipophilic dye DiD (Markosyan et al., 2005 and Experimental Procedures). Fusion with the plasma membrane should lead to the disappearance of the viral membrane and content markers due to their virtually infinite dilution within the plasma membrane and the cytosol, respectively (Figure 2A). In contrast, virus fusion with a small intracellular organelle that is not continuous with the plasma membrane should lead to the loss of viral content without the disappearance of a membrane marker. Hence, the fusion sites can be identified based on the dilution of viral markers.

We validated this strategy by imaging the fusion of pseudoviruses bearing E1/E2 glycoproteins of the low pH-dependent Semliki Forest Virus (SFV). Normally, SFV fuses with acidic endosomes, but it can also be forced to fuse with the plasma membrane by lowering the pH (Marsh and Bron, 1997). As expected, SFV fusion with endosomes resulted in the disappearance of the viral content while the membrane marker remained localized within an endosome (Figure S3A and Movie S1). In contrast, exposure to low pH led to the quick redistribution of viral lipids, but not of viral content (Figure S3B and Movie S2), demonstrating the failure of SFV to undergo full fusion with the plasma membrane.

HIV-1 Fusion with the Plasma Membrane Is Blocked after the Lipid Mixing Stage

JRFL or HXB2 viruses were prebound to TZM-bl cells in the cold and triggered to fuse by quickly shifting to 37°C. We observed three principal outcomes of HIV-cell fusion. First, viruses released their lipid marker, as seen by the disappearance of the red signal, but retained their content for as long as we imaged (Figure 2B and Movie S3). Particles undergoing this type of fusion usually exhibited limited movement before and after the lipid transfer (Figure 2C). These events were almost assuredly due to the partial fusion at the cell surface that did not result in the cytosolic delivery of viral content. Second, following the transport of viruses toward the cell nucleus, typical for endosomal trafficking (Lakadamyali et al., 2004), the viral content marker disappeared while the lipid marker continued to move as a distinct spot (Figures 2D–2G; Movies S4 and S5). These events observed for both JRFL and HXB2 viruses were interpreted as the cytosolic release of viral content through fusion with endosomes. Third, viral markers were released (disappeared) sequentially, often exhibiting a considerable delay between lipid and content transfer (see Figure 5 below). As discussed below,

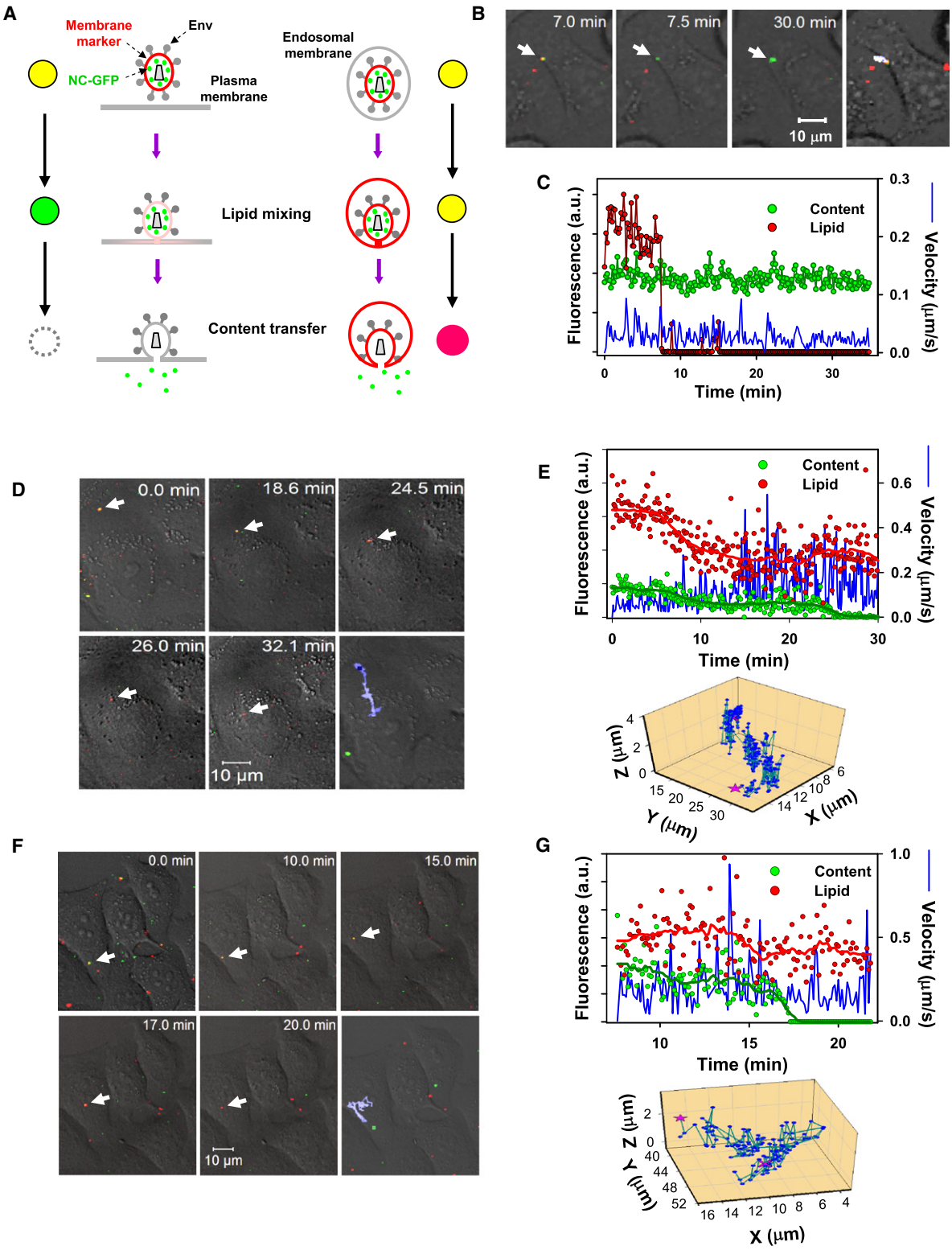

Figure 2. Identification of HIV-1 Fusion Sites by Single-Virus Imaging

(A) Schematic presentation of redistribution of viral lipid and content markers upon fusion with a plasma membrane (left) and with an endosome (right). Viruses colabeled with membrane (red) and content (green) markers are pseudocolored yellow.

these events (hereafter dubbed the two-step fusion) likely reflect the full fusion proceeding in two distinct temporally and, in most cases, spatially separated steps.

JRFL and HXB2 pseudoviruses exhibited distinct fusion phenotypes. The majority of JRFL particles exchanged lipids with the plasma membrane, while the content release from endosomes was less frequent (Figure 3A). By comparison, most HXB2 particles underwent endosomal fusion, very few released the lipid marker, and none exhibited the two-step phenotype seen for JRFL viruses. The overall low probability of HIV-cell fusion is in agreement with our previous data (Markosyan et al., 2005). In control experiments, viral lipid and content transfer was inhibited by a high concentration of C52L (Figure 3A), demonstrating that the overwhelming majority of viral lipid and content transfer events were mediated by HIV-1 Env. Viral content release was not detected between JRFL pseudoviruses and HeLa cells expressing CD4 but not CCR5 (Figure 3A). Thus, under our experimental conditions, the deterioration of the GFP signal caused by low pH in late endosomes/lysosomes was negligible (see also Figure S2C).

The restriction on virus fusion at the cell surface was not limited to HIV-1 and SFV pseudoviruses. We found that the Env glycoprotein of pH-independent amphotropic Murine Leukemia Virus (aMLV) also mediated virus fusion with endosomes. Out of 14 detected events, 11 released their content from endosomes (Figures S3C and S3D), 2 transferred only the lipid marker at the cell surface, and 1 exhibited sequential (two-step) lipid and content release.

Endosomal Fusion Can Lead to Infection

To relate single-virus fusion to infectivity, we evaluated the fraction of cells for which at least one content transfer event was detected by imaging. Endosomal fusion was observed for 8.0% and 10.5% of cells incubated with JRFL and HXB2 particles, respectively (Figure 3B). Under identical conditions, 8.6% of cells were infected by JRFL and 5.7% by HXB2 (i.e., multiplicity of infection [moi] was ~0.1). The fraction of fusion-supporting cells was clearly underestimated due to the missed events. The relatively low fraction of double-labeled particles produced by the labeling protocol and the relatively short imaging time limited our ability to track all fusion events. Nonetheless, comparable efficacies of viral content delivery and infection indicate that a significant fraction of endosomal fusion established productive infection.

Infectious HIV-1 Fuses with an Endosome but Not with the Plasma Membrane

To take advantage of the diffusible NC-GFP marker, our initial imaging experiments employed MLV-based pseudoviruses. To ensure adequate incorporation of HIV-1 Env into these particles, we used the gp41 construct lacking the cytoplasmic domain (Figures S2A and S2B and Markosyan et al., 2005). To rule out the possibility that deletion of the cytoplasmic domain or pseudotyping with the MLV core alters the virus entry sites, we labeled infectious viruses by cotransfecting the cells with the proviral HIV-1 R9 clone encoding a full-length CXCR4-tropic Env (Gallay et al., 1997) and a new vector expressing GFP-tagged HIV Gag. In this construct (referred to as MA-GFP-CA), the EGFP coding sequence (flanked by the viral protease cleavage sites) was inserted between the MA and CA sequences of Gag polyprotein (see Supplemental Experimental Procedures). Upon virus maturation, MA-GFP-CA is cleaved by viral protease, yielding a free GFP (Figures S2F–S2I). These viruses were colabeled with DiD and allowed to fuse with TZM-bl cells.

Similar to pseudovirus fusion, infectious HIV-1 exhibited lipid mixing at the cell surface and content transfer from endosomes (Figures 3A and 3C–3F and Movie S6), whereas the sequential lipid and content release (two-step events, see Figures 5E and 5F) was less frequent. All fusion-related activities were abrogated in the presence of C52L (n = 972). We observed the same fusion phenotype for particles produced by pseudotyping the HIV-1 core with the full-length Env (Figures 3A, S3E, and S3F). Together, these results imply that, irrespective of the origin of the viral core or the presence of the cytoplasmic domain, HIV-1 Env-mediated content delivery into HeLa-derived target cells occurs through fusion with endosomes. Moreover, in CEMss cells, infectious HIV-1 also underwent partial fusion (lipid transfer) with the plasma membrane and complete fusion with endosomes (Figure S4).

Endosomal Fusion Is Delayed Relative to Lipid Transfer at the Cell Surface

The kinetics of single HIV-1 pseudovirus fusion with the plasma membrane and with endosomes was determined by measuring the waiting time from raising the temperature to each lipid or content transfer event, respectively (Figure 4A). Content release from endosomes started after a considerable delay (~10 min), whereas lipid transfer proceeded without an apparent lag. The rates of surface and endosomal fusion differed markedly regardless of the virus tropism (JRFL versus HXB2) and regardless of whether MLV core-based pseudoviruses or infectious HIV-1 viruses (Figure 4C) were imaged. The delayed release of the viral content marker is consistent with the lag in the cytosolic BlaM delivery measured by the TB protocol (Figure 1A). In fact, after renormalization to correct for the shorter imaging time, the rates of viral content delivery measured by single-virus and BlaM assays were indistinguishable (Figure S5). This finding validates the usage of the TB protocol for measuring the rate of formation of relatively small fusion pores and implies that complete pore dilation is not required for detecting the BlaM signal in the cytosol.

(B and C) Partial fusion of JRFL with the plasma membrane of TZM-bl cells. The time from the beginning of imaging is shown. The two-dimensional projection of the particle's trajectory (cyan) is overlaid on the last image. Changes in fluorescence intensities (in arbitrary units) of membrane (red) and content (green) markers, as well as the instantaneous velocity (blue trace) of the particle, are shown.

(D–G) Complete fusion of JRFL (D and E) and HXB2 (F and G) viruses following the fast retrograde movement from the cell periphery (cyan traces on last images). Fusion is evident from the disappearance of GFP signal. Graphs (E and G) show changes in fluorescence of membrane and content markers (smoothed for visual clarity) and 3D trajectories for the viruses marked by arrows in (D) and (F). See Movies S3–S5.

A

Virus	Lipid transfer (%)	Content release (%)	Two-step events (%)
JRFL/MLV (HeLa-CD4) n=1061	0.2	0	0
JRFL/MLV n=3647	3.9 (0.3)	1 (0.15)	0.8 (0.0)
JRFL/HIV n=496	1.4 (ND)	2.2 (ND)	0 (ND)
HXB2/MLV n=2117	0.3 (0)	1.8 (0.2)	0 (0)
R9 n=2037	0.9 (0)	1.2 (0)	0.2 (0)

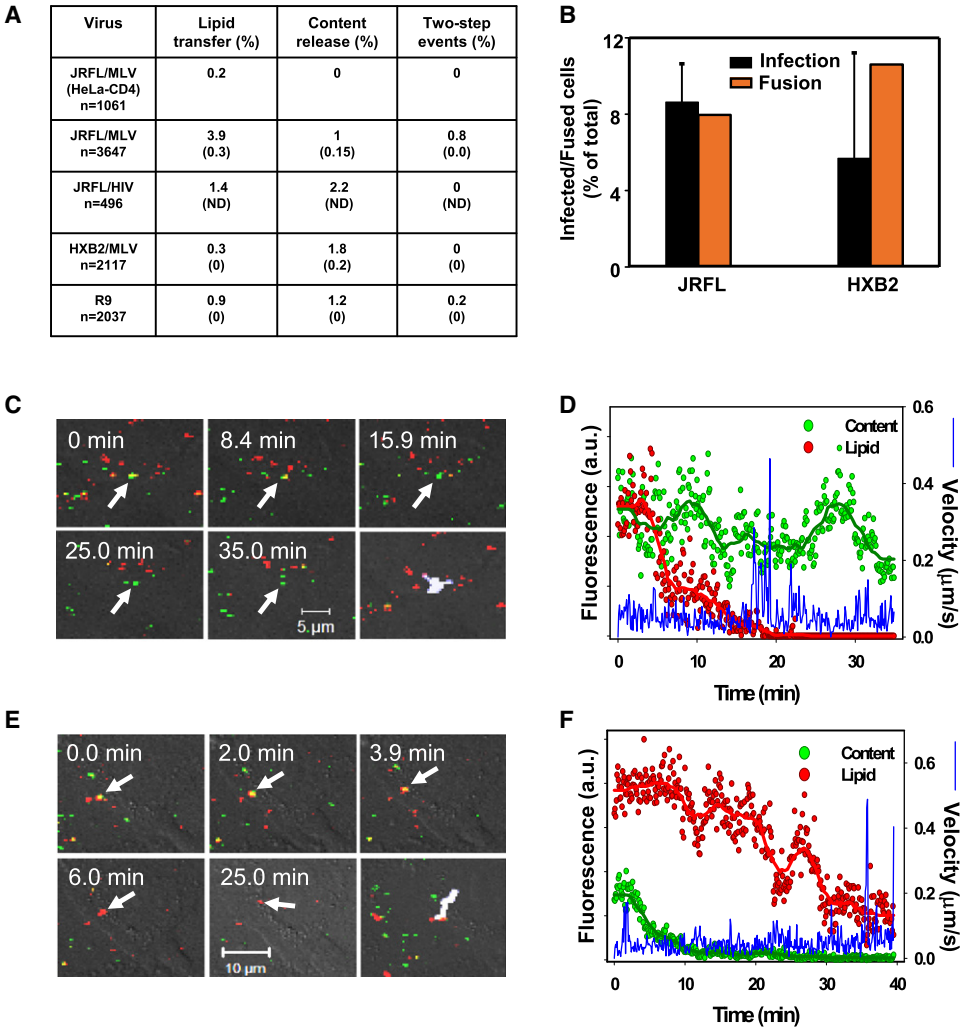

Figure 3. Fusion of HIV Core-Based Pseudoviruses and of Infectious HIV-1 with TZM-bl Cells

(A) The efficiency of lipid mixing with the plasma membrane, the viral content release from endosomes, and the sequential two-step fusion events mediated by JRFL Env (pseudotyped with MLV or HIV core), HXB2 Env, and infectious R9 viruses. The first row is the negative control for JRFL fusion using HeLa-CD4 cells lacking CCR5. The number of respective fusion-related events was normalized to the total number of cell-associated double-labeled virions at the beginning of the experiment. The extents of viral lipid and content mixing in the presence of 4 μM C52L are shown in parentheses. The rare false-positive events in the presence of C52L were usually delayed relative to those in the absence of the inhibitor (data not shown) and were minimized by limiting the duration of imaging experiments. ND, not determined.

(B) The fraction of cells supporting viral content release was measured by imaging (orange bars), and the fraction of infected cells in the same sample was determined by a β-gal assay (black bars) after an additional 48 hr cultivation in the presence of C52L. The somewhat larger fraction of cells supporting HXB2 fusion was due to a more efficient binding of HXB2 to target cells compared to JRFL viruses (data not shown). Error bars are SEM (n = 3).

(C and D) Lipid transfer initiated by the infectious R9 HIV-1 labeled with DiD and MA-GFP-CA at the surface of the TZM-bl cell.

(E and F) Complete endosomal fusion of the infectious R9 particle. See Movie S6.

HIV-1 Fusion May Proceed through a Stable Hemifusion-like Intermediate

Even though the loss of a lipid marker during the two-step fusion precludes unambiguous determination of the site of subsequent content release, the latter step appears to occur in endosomes. First, the rates of sequential lipid and content transfer for the two-step fusion were statistically indistinguishable ($p > 0.180$ and $p > 0.594$, respectively) from the respective rates of separate surface and endosomal fusion events (Figure 4B). Hence, by analogy to endosomal fusion, the content release through the two-step events likely occurs in endosomes. This result also implies that the two-step events are a subset of "regular" fusion events, in which lipid transfer occurred prior to virus uptake. Second, the pronounced delay between lipid and content transfer during the two-step events (half-time of about 10 min, Figure 4B) was sufficiently long to permit virus endocytosis ($t_{1/2}$ = 13.5 min, Figure 1A) prior to content release.

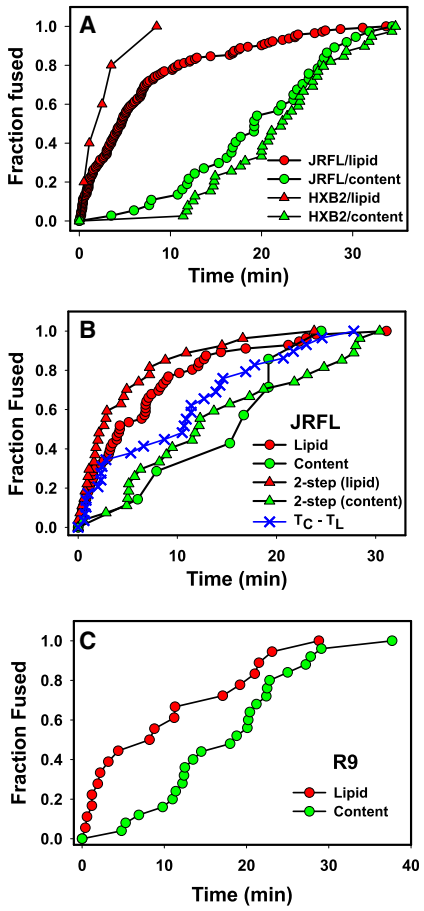

Figure 4. Lipid Mixing at the Cell Surface Precedes the Content Release from Endosomes

(A) The kinetics of JRFL (circles) and HXB2 (triangles) fusion with TZM-bl cells. Waiting times from the shift to 37°C to the point of lipid (red symbols) or content (green symbols) transfer were measured, rank ordered, and plotted as cumulative distributions of the fraction of fused viruses over time.

(B) Comparative kinetics of partial fusion at the cell surface (red circles), endosomal fusion (green circles), and sequential lipid and content transfer exhibited during the two-step events (red and green triangles, respectively). The time intervals between sequential lipid (T_L) and content (T_C) transfer were ranked and plotted as cumulative distribution (crosses).

(C) The kinetics of lipid and content mixing during fusion of infectious R9 HIV-1 viruses with TZM-bl cells.

Third, by tracking the two-step fusion events, we found that viruses tended to accelerate (>0.2 μm/s) prior to or at the time of content release (Figures 5A and 5B). These particles were thus judged to have entered an endocytic pathway and fused with endosomes. Only 1 out of 22 particles released approximately half of its content (Figures 5C and 5D, arrow) without a significant prior displacement. However, the incomplete release of viral content shows that, even if this fusion pore was formed at the cell surface, it closed soon after opening (schematically shown by the thick line above Figure 5D). Importantly, viral content release did not resume until after the onset of fast movement (double arrow and Movie S7) associated with virus uptake. We also found that the content release during the two-step events exhibited by infectious HIV-1 usually coincided with the fast particle movement (Figures 5E and 5F).

These data imply that, even when HIV-1 establishes lipid continuity with the plasma membrane, it fails to form a fusion pore that permits the transfer of a content marker. This fusion phenotype is operationally defined as membrane hemifusion (Chernomordik and Kozlov, 2005). The temporal separation of lipid and content transfer events suggests that the two-step fusion proceeds through a remarkably long-lived hemifusion intermediate. We cannot rule out the possibility that the lipid mixing at the cell surface represents a nonproductive pathway, in which case, distinct Env trimers would be responsible for subsequent endosomal fusion. However, given the paucity of Env trimers in HIV-1 particles (Zhu et al., 2006), formation of more than one fusion complex per virion appears unlikely, suggesting that hemifusion is a bona fide intermediate of HIV entry.

Clathrin- and Dynamin-Dependent Endocytosis Is a Prerequisite for HIV-1 Fusion

To obtain further evidence that HIV-1 is internalized prior to fusion, we blocked clathrin- and caveolin-mediated endocytosis by pretreating the TZM-bl cells with dynasore, a small-molecule inhibitor of the dynamin GTPase activity that prevents the scission of clathrin-coated pits from the plasma membrane (Macia et al., 2006). At a concentration that blocked transferrin uptake (Figure S7A), dynasore diminished virus internalization and strongly inhibited HIV-1 infection and fusion with TZM-bl and CEMss cells (Figures 6A and 6B, respectively). As expected for viruses entering cells via a clathrin-dependent pathway (Sun et al., 2005), fusion and infection by VSV G pseudoviruses were suppressed by the drug. The diminished HIV-1 fusion was not caused by the downregulation of CD4 or CR expression, reduction of virus binding, or the compromised ability of Env to promote fusion in the presence of dynasore (Figures S7B–S7D).

To control against possible adverse effects of dynasore, we assessed the effect of MiTMAB, a surface-active inhibitor that blocks dynamin's interactions with phospholipids (Quan et al., 2007). The diminished HIV-1 fusion in cells pretreated with MiTMAB (Figure 6C) supported the essential role of dynamin in virus entry. By comparison, the small-molecule inhibitor of Cdc42 GTPase, secramine A (Pelish et al., 2006), augmented HIV-1 fusion. The specificity of small-molecule dynamin inhibitors was further verified by showing that HIV-1 fusion was suppressed in cells overexpressing the dominant-negative K44A mutant of dynamin (Damke et al., 1994) (Figure S8). These results, along with the inhibition of HIV-1 fusion by a hypertonic medium (Figure 6C) known to inhibit clathrin-mediated endocytosis, suggest that HIV-1 is internalized via a clathrin-dependent pathway prior to undergoing fusion.

To determine which step of HIV fusion is blocked by dynasore, we performed single-virus imaging experiments. Viruses bound to cells pretreated with the drug exhibited highly restricted mobility compared to control experiments (data not shown), consistent with inhibited virus endocytosis. Most importantly, dynasore abolished the viral content release but permitted the lipid transfer to the plasma membrane (Figure 6G). In the absence of virus uptake, partial fusion at the cell surface led to

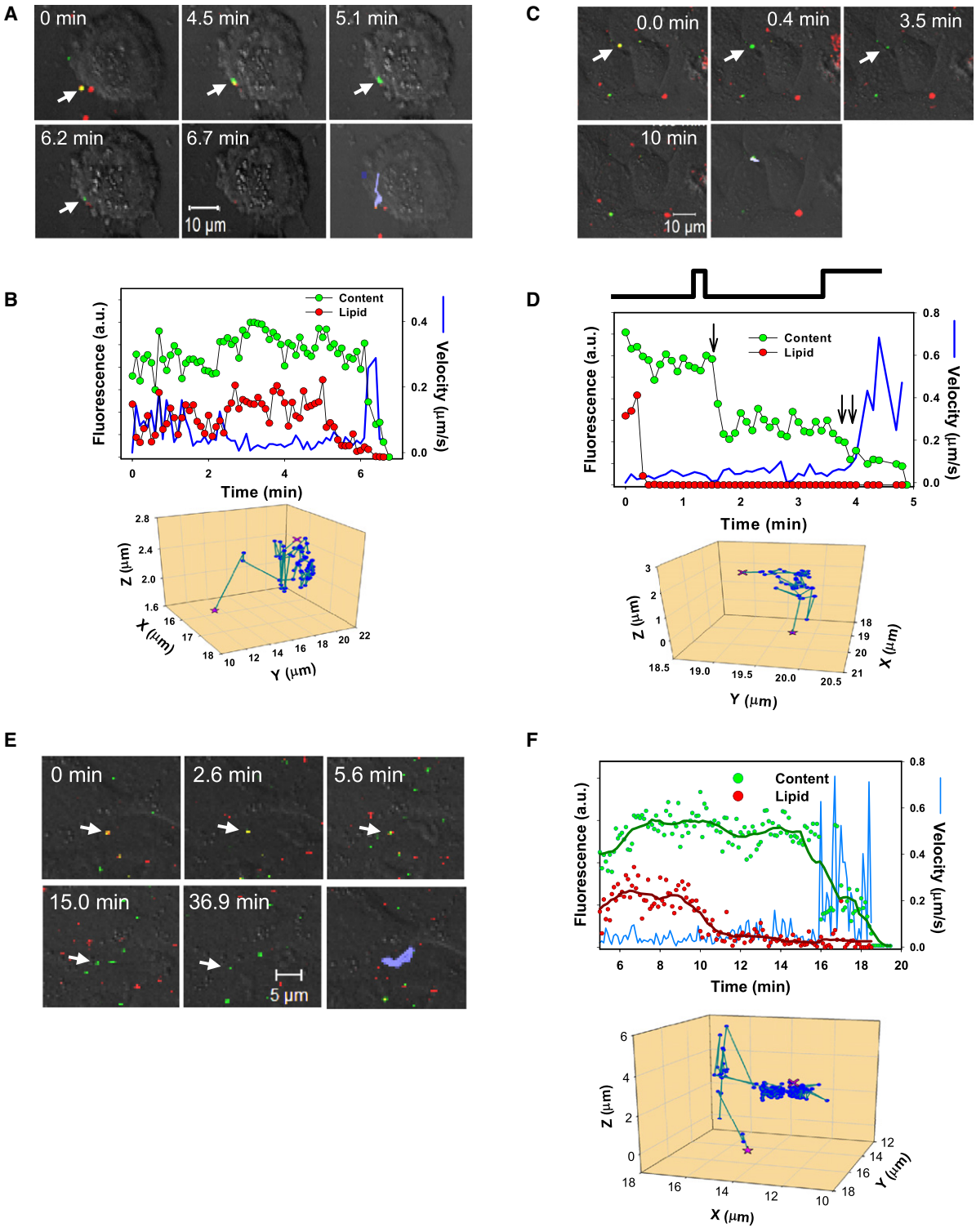

Figure 5. Sequential Lipid and Content Transfer Events Exhibited by HIV-1

(A and B) A two-step fusion event exhibiting a short delay between lipid and content transfer.

(C and D) A rare two-step event characterized by stepwise release of viral content. Complete content discharge (double arrow) occurs after the onset of quick movement (see Movie S7). The predicted dynamics of a fusion pore (D) is shown by a thick line above the panel. The initial and final coordinates of particles on 3D plots are marked by pink crosses and stars, respectively.

(E and F) The two-step fusion of infectious R9 HIV-1 colabeled with DiD and MA-GFP-CA. Changes in fluorescence intensities of viral lipid and content markers upon incubation with TZM-bl cells at 37°C are smoothed for visual clarity.

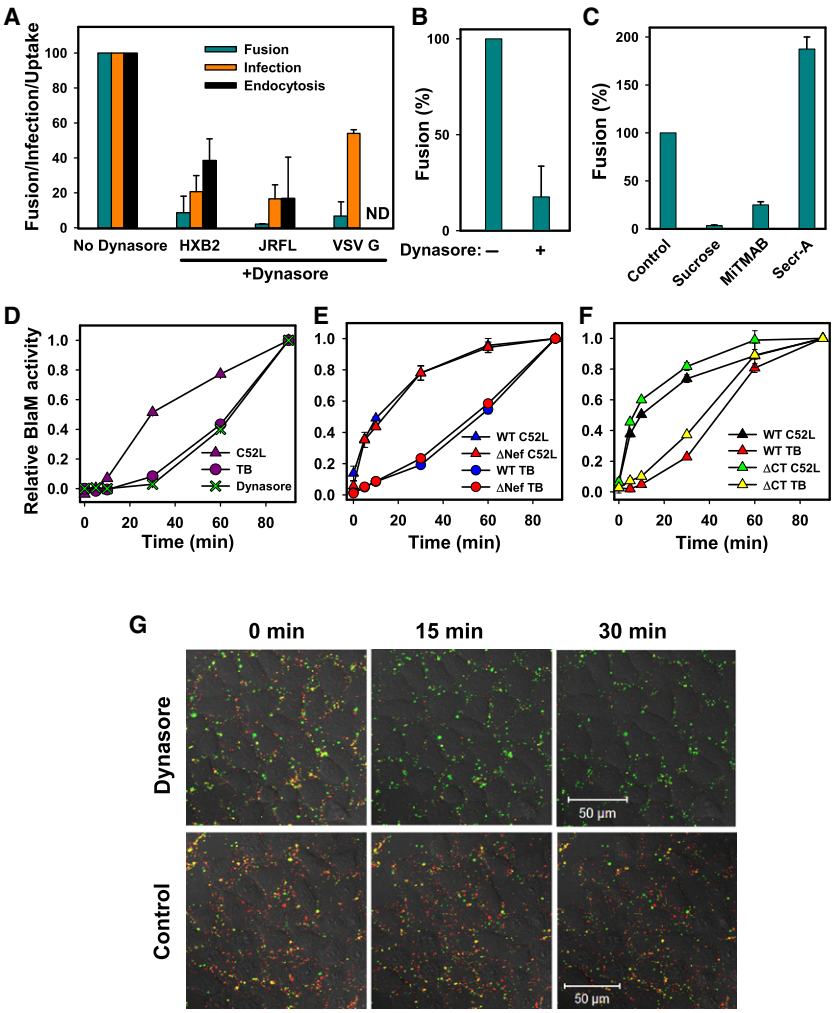

Figure 6. Blocking the Dynamin Function Inhibits HIV-1 Uptake, Fusion, and Infection

(A) TZM-bl cells were pretreated with 80 μM dynasore and allowed to bind viruses in the cold. Virus uptake after a 1 hr incubation at 37°C was measured by the accumulation of intracellular p24 (black bars, n = 6), as described in the Supplemental Experimental Procedures. The extent of fusion was quantified by the BlaM assay (dark cyan bars, n = 4), and single-cycle infection was measured by a β-gal assay (orange bars, n = 6).

(B) Inhibition of HXB2 fusion with CEMss cells pretreated with dynasore.

(C) Inhibition of HXB2 fusion in TZM-bl cells pretreated with 0.45 M sucrose, 80 μM MiTMAB, and 15 μM secramine A.

(D) The kinetics of HXB2 escape from 80 μM dynasore added at indicated times of incubation at 37°C. The background fusion (~20% of total) in the presence of dynasore was subtracted from the dynasore curve to ease the comparison with the C52L and TB curves.

(E) Fusion of wild-type (WT) and Nef-deficient (ΔNef) viruses bearing HXB2 Env with TZM-bl cells.

(F) Kinetics of fusion mediated by the wild-type and cytoplasmic tail-deleted (ΔCT) JRFL Env.

(G) Pretreatment of TZM-bl cells with dynasore blocks the HXB2 content (NC-GFP) transfer but permits lipid transfer (disappearance of DiD) to the plasma membrane. The loss of the red signal was due in part (~50%) to dynasore directly quenching the DiD fluorescence (data not shown).

Unless indicated otherwise, error bars are SEM (n ≥ 3).

HIV inactivation, as evidenced by the lack of recovery of the BlaM signal after the removal of dynasore (Figure S7E). These results confirm that HIV-1 is unable to fuse at the cell surface and that the fusion block occurs after the lipid mixing stage.

Endocytosis Reduces the Window of Opportunity for the Inhibitory Peptide to Bind to Intermediate Conformations of gp41

Clearance from the cell surface prior to the completion of fusion can protect HIV-1 against antibodies and inhibitors targeting Env epitopes that are exposed during the slow fusion reaction. To test this notion, we sought to reversibly slow down virus uptake while permitting its interactions with CD4 and CR. After unsuccessful attempts to reversibly arrest virus uptake using different intervention strategies, we chose to create a temperature-arrested stage (TAS) that has been described before (Henderson and Hope, 2006; Mkrtchyan et al., 2005). After binding to cells in the cold, the viruses/cells were incubated for several hours at a temperature that minimized productive endocytosis and virus-cell fusion (for details, see the legend to Figure S6). This intermediate stage was reversible, as fusion quickly ensued upon raising the temperature (Figures S6A and S6C). At this stage, a fraction of fusion events became resistant to CD4- and CR-binding inhibitors, demonstrating the formation of ternary complexes, which in turn resulted in the exposure of the gp41 coiled-coil regions targeted by inhibitory peptides, such as T20 and C34 (Eckert and Kim, 2001). We were thus able to control the exposure of pretriggered gp41 to C34 by varying the interval between adding this peptide at the TAS and inducing endocytosis (and fusion) by shifting to 37°C. The longer exposure to C34 enhanced its inhibitory activity (Figures S6B and S6D), consistent with the notion that endocytic entry of HIV-1 might attenuate the potency of this class of fusion inhibitors.

HIV-Endosome Fusion Does Not Rely on an Intact Cytoskeleton but Depends on Dynamin Activity

The reliance of HIV-1 fusion on endosomal pathways prompted us to examine the effects of actin- and microtubule-disrupting agents also known to interfere with endosomal trafficking and maturation (Bayer et al., 1998). Pretreatment of cells with latrunculin A or nocodazole led to a modest reduction of the extent but not the rate of HIV-1 fusion (Figure S9). This finding indicates that the BlaM signal is not critically affected by actin- and microtubule-dependent processes, in agreement with the previous work (Campbell et al., 2004).

Dynasore's ability to quickly block endocytosis (Macia et al., 2006 and Figure S7F) permitted us to perform time-of-addition experiments and delineate the step(s) of HIV-1 fusion sensitive

to this compound. Dynasore was added after varied times of virus-cell incubation, and the drug-resistant fusion was compared to that obtained by the C52L and TB protocols. The loss of sensitivity to inhibitors of virus endocytosis is expected to occur at the time of the virus' escape from C52L. Remarkably, however, HIV-1 escape from dynasore was markedly delayed and was indistinguishable from its escape from the TB (Figure 6D). This finding indicates that dynamin plays a role both in HIV-1 uptake and in virus-endosome fusion.

Next, we asked whether dynamin-2 could augment Env-mediated fusion with endosomes through its specific binding to the accessory HIV-1 Nef protein (Pizzato et al., 2007) exposed to the cytosol as a result of fusion. However, the identical rates (Figure 6E) and extents (data not shown) of fusion of wild-type and Nef-deficient viruses did not support this possibility. Thus dynamin appears to promote HIV-1 fusion indirectly, perhaps by interacting with effector protein(s) involved in a variety of cellular processes, such as cytokinesis, membrane trafficking, cell migration, and adhesion (Kim and Chang, 2006; Kruchten and McNiven, 2006; Peters et al., 2004). We also tested whether the unusually long cytoplasmic domain of gp41 is involved in pore formation or dilation either directly or by interacting with its cellular partners. Deletion of the cytoplasmic domain did not considerably alter the kinetics of viral escape from the TB relative to its escape from C52L (Figure 6F), implying that this domain is not essential for HIV-1 fusion.

DISCUSSION

Time-resolved imaging of single viruses and differential blocking of fusion by site-specific and universal inhibitors revealed that HIV-1 co-opts the endocytic machinery to enter into and fuse with target cells. By contrast, fusion with the plasma membrane did not progress beyond the lipid mixing step, suggesting that endosomal entry is the pathway that leads to productive infection. Endocytic entry offers several advantages, including the sheltering of HIV-1 from antibodies and inhibitors targeting intermediate conformations of Env during the unusually slow fusion reaction. Indeed we found that the delayed virus uptake increased the potency of the inhibitory C34 peptide. Thus, in order to efficiently block intracellular fusion events, the next generation of HIV entry inhibitors must be able to permeate the cell membrane.

The failure of HIV to fuse with the plasma membrane is in stark contrast to cell-cell fusion mediated by Env glycoproteins of this and other pH-independent viruses. While the basis for this discrepancy is unclear, the much larger number of Env involved in cell-cell contact compared to a few Env responsible for virus entry could increase the likelihood of fusion at the cell surface. Another manifestation of differences between these experimental systems is the prolonged lag between CD4/CR-mediated HIV-1 uptake and endosomal fusion. By comparison, the formation of ternary Env-CD4-CR complexes abrogated the lag before cell-cell fusion (Melikyan et al., 2000; Mkrtchyan et al., 2005). The delayed endosomal fusion of HIV-1 is indicative of a rate-limiting step downstream of coreceptor-dependent steps and downstream of a hemifusion-like intermediate. Slow pore enlargement is unlikely to contribute to this delay because both single-virus imaging and the BlaM assay appear to detect relatively small pores. It is thus possible that the formation of higher-order Env oligomers and/or gp41 folding into the 6-helix bundle are rate-limiting for HIV-cell fusion. Alternatively, the lag before fusion could reflect the time required for HIV-1 delivery into permissive intracellular compartments, such as late endosomes.

Accumulating evidence suggests that entry of viruses other than HIV-1 by direct fusion with the plasma membrane is also disfavored. For instance, pH-independent MLV and respiratory syncytial virus appear to utilize an endocytic pathway for infection (Beer et al., 2005; Katen et al., 2001; Kolokoltsov et al., 2007). Infection by several low pH-dependent viruses can be hindered when fusion with a plasma membrane is forced by acidic pH (Marsh and Bron, 1997; Matlin et al., 1982; Mothes et al., 2000). The failure of HIV-1, aMLV, and SFV to progress beyond the lipid mixing step at the cell surface (Figures 2, 3, and S3) shows that the block for pH-dependent and pH-independent infection is at the stage of formation and/or dilation of a fusion pore. The lack of complete fusion at the cell surface could be due to restrictions imposed by the cortical actin or other factors present in or around the plasma membrane. However, the modest effect of actin depolymerization on viral content delivery (Figure S9) does not support this notion. An alternative possibility discussed below is that viruses rely on yet unidentified endosomal factors to promote complete fusion.

Our data revealed a novel role for dynamins in HIV-1 content release from endosomes. Why would HIV-1 need cellular factors to promote fusion? Several lines of evidence suggest that the formation and enlargement of a fusion pore are the most energy-intensive steps (reviewed in Melikyan, 2008) that require the concerted action of several viral proteins. Considering the low number of Env per virion (Zhu et al., 2006), HIV-1 may not be able to sustain a fusion pore on its own without cellular partners. The ability of dynamin to regulate actin remodeling and/or to associate with membrane-bending proteins (Kruchten and McNiven, 2006) could provide an additional driving force to expand pores and permit the release of the HIV-1 core. It is thus possible that cellular factors involved in membrane trafficking are responsible for the virus' strong preference for endocytic entry.

EXPERIMENTAL PROCEDURES

BlaM Assay for Virus-Cell Fusion

TZM-bl cells ($4 \cdot 10^4$ cells/well) were grown overnight in 96-well plates in a phenol red-free growth medium. Viruses were added to cells at moi 0.7–1.0 and centrifuged at 2095 g, 4°C for 30 min. The cells were washed with a cold medium to remove free viruses, and fusion was initiated by shifting to 37°C. After an indicated time at 37°C, fusion was stopped by adding C52L (1 μM) or other fusion inhibitors. All samples were maintained at 37°C for a total of 90 min (unless indicated otherwise), chilled by briefly placing on ice, loaded with the CCF2-AM substrate (GeneBLAzer in vivo Detection Kit, Invitrogen), and incubated overnight at 13.5°C (or as indicated). In the temperature block protocol, cells were placed on ice until the end of the experiment and then loaded with the BlaM substrate. Fusion of HIV-1 pseudotyped with VSV G was carried out as described above but stopped at indicated times by either treating cells with pronase, placing cells on ice (TB), or adding 50 mM NH_4Cl. The temperature chase experiments were carried out by introducing C52L peptide after 20 min of incubation, as in the standard fusion protocol. The BlaM signal was then chased by placing cells on ice either immediately

or at the indicated times of incubation at 37°C in the presence of C52L. The BlaM activity was quantified using Synergy HT fluorescence plate reader (Bio-Tek Instr., Germany). The extent of virus-cell fusion was determined from the ratio of blue (440–480 nm) and green (518–538 nm) emission upon exciting the cells at 405–415 nm. HIV-1 fusion with CEMss cells was carried out by resuspending the cells in media containing HXB2 pseudoviruses (moi 1–1.5) and centrifuging at 2095 g, 4°C for 30 min. The free viruses were washed off, and fusion was initiated by shifting to 37°C and stopped after indicated times either by adding C52L peptide or by placing cells on ice. The cells were then loaded with the CCF2-AM substrate and transferred into a 96-well plate ($1 \cdot 10^5$ cells/well), and the BlaM activity was determined as described above.

Single-Particle Imaging and Analysis

Viruses were centrifuged onto TZM-bl cells cultured on a cover glass (2095 g for 1 hr at 12°C). The cells were washed to remove unbound viruses and transferred into an imaging chamber. Virus-cell fusion was triggered by quickly and locally raising the temperature to 37°C using a home-built temperature-jump setup (Melikyan et al., 2000) and visualized using a Zeiss LSM 510 Meta confocal microscope. Unless noted otherwise, samples were simultaneously excited at 488 and 633 nm, and the emitted light was collected by a C-Apo 40×/1.2 water immersion or a Neofluar 40×/1.3 oil immersion objective, split, and passed through 505–550 nm band-pass and 650 nm long-pass filters. To minimize photobleaching, only 3–4 Z stacks spaced by 2.5 μm were acquired every 6–7 s for 35–40 min. Single-particle tracking was performed using Volocity image analysis software (Improvision, Perkin Elmer). Briefly, the total number of cell-associated viruses containing detectable amounts of DiD and GFP-based content marker was determined by identifying contiguous pixels with fluorescence intensity at least 3-fold greater than background. The waiting times for fusion were estimated as the time interval from raising the temperature to 37°C to the point when the signal from either the membrane or content marker dropped to the background level. Three-dimensional tracking of particles over time was performed by adjusting the intensity threshold and the maximal particle displacement between consecutive frames.

SUPPLEMENTAL DATA

Supplemental Data include Supplemental Experimental Procedures, nine figures, and seven movies and can be found with this article online at http://www.cell.com/supplemental/S0092-8674(09)00268-2.

ACKNOWLEDGMENTS

The authors are grateful to Dr. T. Kirchhausen for dynasore and to Drs. C. Aiken, M. Alizon, J. Binley, J. Cunningham, M. Kielian, G. Lewis, M. Lu, W. Mothes, J. Strizki, L. Wang, and J. Young, as well as the NIH AIDS Research and Reference Reagent Program for reagents, expression vectors, and cell lines. We thank Dr. M. Reitz for his help in designing the MA-GFP-CA construct and Drs. L. Chernomordik and R. Dutch for stimulating discussions. This work was supported by NIH R01 GM054787 and AI053668 grants to G.B.M. Y.K. was partially supported by the SDG from the American Heart Association.

Received: October 17, 2008
Revised: January 3, 2009
Accepted: February 25, 2009
Published: April 30, 2009

REFERENCES

Aiken, C. (1997). Pseudotyping human immunodeficiency virus type 1 (HIV-1) by the glycoprotein of vesicular stomatitis virus targets HIV-1 entry to an endocytic pathway and suppresses both the requirement for Nef and the sensitivity to cyclosporin A. J. Virol. *71*, 5871–5877.

Bayer, N., Schober, D., Prchla, E., Murphy, R.F., Blaas, D., and Fuchs, R. (1998). Effect of bafilomycin A1 and nocodazole on endocytic transport in HeLa cells: implications for viral uncoating and infection. J. Virol. *72*, 9645–9655.

Beer, C., Andersen, D.S., Rojek, A., and Pedersen, L. (2005). Caveola-dependent endocytic entry of amphotropic murine leukemia virus. J. Virol. *79*, 10776–10787.

Brandt, S.M., Mariani, R., Holland, A.U., Hope, T.J., and Landau, N.R. (2002). Association of chemokine-mediated block to HIV entry with coreceptor internalization. J. Biol. Chem. *277*, 17291–17299.

Campbell, E.M., Nunez, R., and Hope, T.J. (2004). Disruption of the actin cytoskeleton can complement the ability of Nef to enhance human immunodeficiency virus type 1 infectivity. J. Virol. *78*, 5745–5755.

Cavrois, M., De Noronha, C., and Greene, W.C. (2002). A sensitive and specific enzyme-based assay detecting HIV-1 virion fusion in primary T lymphocytes. Nat. Biotechnol. *20*, 1151–1154.

Cavrois, M., Neidleman, J., Yonemoto, W., Fenard, D., and Greene, W.C. (2004). HIV-1 virion fusion assay: uncoating not required and no effect of Nef on fusion. Virology *328*, 36–44.

Chernomordik, L.V., and Kozlov, M.M. (2005). Membrane hemifusion: crossing a chasm in two leaps. Cell *123*, 375–382.

Daecke, J., Fackler, O.T., Dittmar, M.T., and Krausslich, H.G. (2005). Involvement of clathrin-mediated endocytosis in human immunodeficiency virus type 1 entry. J. Virol. *79*, 1581–1594.

Damke, H., Baba, T., Warnock, D.E., and Schmid, S.L. (1994). Induction of mutant dynamin specifically blocks endocytic coated vesicle formation. J. Cell Biol. *127*, 915–934.

Deng, Y., Zheng, Q., Ketas, T.J., Moore, J.P., and Lu, M. (2007). Protein design of a bacterially expressed HIV-1 gp41 fusion inhibitor. Biochemistry *46*, 4360–4369.

Doms, R.W., and Trono, D. (2000). The plasma membrane as a combat zone in the HIV battlefield. Genes Dev. *14*, 2677–2688.

Eckert, D.M., and Kim, P.S. (2001). Mechanisms of viral membrane fusion and its inhibition. Annu. Rev. Biochem. *70*, 777–810.

Fredericksen, B.L., Wei, B.L., Yao, J., Luo, T., and Garcia, J.V. (2002). Inhibition of endosomal/lysosomal degradation increases the infectivity of human immunodeficiency virus. J. Virol. *76*, 11440–11446.

Frey, S., Marsh, M., Gunther, S., Pelchen-Matthews, A., Stephens, P., Ortlepp, S., and Stegmann, T. (1995). Temperature dependence of cell-cell fusion induced by the envelope glycoprotein of human immunodeficiency virus type 1. J. Virol. *69*, 1462–1472.

Gallay, P., Hope, T., Chin, D., and Trono, D. (1997). HIV-1 infection of nondividing cells through the recognition of integrase by the importin/karyopherin pathway. Proc. Natl. Acad. Sci. USA *94*, 9825–9830.

Henderson, H.I., and Hope, T.J. (2006). The temperature arrested intermediate of virus-cell fusion is a functional step in HIV infection. Virol. J. *3*, 36.

Katen, L.J., Januszeski, M.M., Anderson, W.F., Hasenkrug, K.J., and Evans, L.H. (2001). Infectious entry by amphotropic as well as ecotropic murine leukemia viruses occurs through an endocytic pathway. J. Virol. *75*, 5018–5026.

Kim, Y., and Chang, S. (2006). Ever-expanding network of dynamin-interacting proteins. Mol. Neurobiol. *34*, 129–136.

Kolokoltsov, A.A., Deniger, D., Fleming, E.H., Roberts, N.J., Jr., Karpilow, J.M., and Davey, R.A. (2007). Small interfering RNA profiling reveals key role of clathrin-mediated endocytosis and early endosome formation for infection by respiratory syncytial virus. J. Virol. *81*, 7786–7800.

Kruchten, A.E., and McNiven, M.A. (2006). Dynamin as a mover and pincher during cell migration and invasion. J. Cell Sci. *119*, 1683–1690.

Lakadamyali, M., Rust, M.J., and Zhuang, X. (2004). Endocytosis of influenza viruses. Microbes Infect. *6*, 929–936.

Macia, E., Ehrlich, M., Massol, R., Boucrot, E., Brunner, C., and Kirchhausen, T. (2006). Dynasore, a cell-permeable inhibitor of dynamin. Dev. Cell *10*, 839–850.

Maddon, P.J., McDougal, J.S., Clapham, P.R., Dalgleish, A.G., Jamal, S., Weiss, R.A., and Axel, R. (1988). HIV infection does not require endocytosis of its receptor, CD4. Cell *54*, 865–874.

Marechal, V., Prevost, M.C., Petit, C., Perret, E., Heard, J.M., and Schwartz, O. (2001). Human immunodeficiency virus type 1 entry into macrophages mediated by macropinocytosis. J. Virol. *75*, 11166–11177.

Markosyan, R.M., Cohen, F.S., and Melikyan, G.B. (2005). Time-resolved imaging of HIV-1 Env-mediated lipid and content mixing between a single virion and cell membrane. Mol. Biol. Cell *16*, 5502–5513.

Marsh, M., and Bron, R. (1997). SFV infection in CHO cells: cell-type specific restrictions to productive virus entry at the cell surface. J. Cell Sci. *110*, 95–103.

Marsh, M., and Helenius, A. (2006). Virus entry: open sesame. Cell *124*, 729–740.

Matlin, K.S., Reggio, H., Helenius, A., and Simons, K. (1982). Pathway of vesicular stomatitis virus entry leading to infection. J. Mol. Biol. *156*, 609–631.

McClure, M.O., Marsh, M., and Weiss, R.A. (1988). Human immunodeficiency virus infection of CD4-bearing cells occurs by a pH-independent mechanism. EMBO J. *7*, 513–518.

Melikyan, G.B. (2008). Common principles and intermediates of viral protein-mediated fusion: the HIV-1 paradigm. Retrovirology *5*, 111.

Melikyan, G.B., Markosyan, R.M., Hemmati, H., Delmedico, M.K., Lambert, D.M., and Cohen, F.S. (2000). Evidence that the transition of HIV-1 gp41 into a six-helix bundle, not the bundle configuration, induces membrane fusion. J. Cell Biol. *151*, 413–424.

Mkrtchyan, S.R., Markosyan, R.M., Eadon, M.T., Moore, J.P., Melikyan, G.B., and Cohen, F.S. (2005). Ternary complex formation of human immunodeficiency virus type 1 Env, CD4, and chemokine receptor captured as an intermediate of membrane fusion. J. Virol. *79*, 11161–11169.

Mothes, W., Boerger, A.L., Narayan, S., Cunningham, J.M., and Young, J.A.T. (2000). Retroviral entry mediated by receptor priming and low pH triggering of an envelope glycoprotein. Cell *103*, 679–689.

Pauza, C.D., and Price, T.M. (1988). Human immunodeficiency virus infection of T cells and monocytes proceeds via receptor-mediated endocytosis. J. Cell Biol. *107*, 959–968.

Pelchen-Matthews, A., Clapham, P., and Marsh, M. (1995). Role of CD4 endocytosis in human immunodeficiency virus infection. J. Virol. *69*, 8164–8168.

Pelish, H.E., Peterson, J.R., Salvarezza, S.B., Rodriguez-Boulan, E., Chen, J.L., Stamnes, M., Macia, E., Feng, Y., Shair, M.D., and Kirchhausen, T. (2006). Secramine inhibits Cdc42-dependent functions in cells and Cdc42 activation in vitro. Nat. Chem. Biol. *2*, 39–46.

Peters, C., Baars, T.L., Buhler, S., and Mayer, A. (2004). Mutual control of membrane fission and fusion proteins. Cell *119*, 667–678.

Pizzato, M., Helander, A., Popova, E., Calistri, A., Zamborlini, A., Palu, G., and Gottlinger, H.G. (2007). Dynamin 2 is required for the enhancement of HIV-1 infectivity by Nef. Proc. Natl. Acad. Sci. USA *104*, 6812–6817.

Quan, A., McGeachie, A.B., Keating, D.J., van Dam, E.M., Rusak, J., Chau, N., Malladi, C.S., Chen, C., McCluskey, A., Cousin, M.A., and Robinson, P.J. (2007). Myristyl trimethyl ammonium bromide and octadecyl trimethyl ammonium bromide are surface-active small molecule dynamin inhibitors that block endocytosis mediated by dynamin I or dynamin II. Mol. Pharmacol. *72*, 1425–1439.

Schaeffer, E., Soros, V.B., and Greene, W.C. (2004). Compensatory link between fusion and endocytosis of human immunodeficiency virus type 1 in human CD4 T lymphocytes. J. Virol. *78*, 1375–1383.

Stein, B.S., Gowda, S.D., Lifson, J.D., Penhallow, R.C., Bensch, K.G., and Engleman, E.G. (1987). pH-independent HIV entry into CD4-positive T cells via virus envelope fusion to the plasma membrane. Cell *49*, 659–668.

Sun, X., Yau, V.K., Briggs, B.J., and Whittaker, G.R. (2005). Role of clathrin-mediated endocytosis during vesicular stomatitis virus entry into host cells. Virology *338*, 53–60.

Wei, B.L., Denton, P.W., O'Neill, E., Luo, T., Foster, J.L., and Garcia, J.V. (2005). Inhibition of lysosome and proteasome function enhances human immunodeficiency virus type 1 infection. J. Virol. *79*, 5705–5712.

Wei, X., Decker, J.M., Liu, H., Zhang, Z., Arani, R.B., Kilby, J.M., Saag, M.S., Wu, X., Shaw, G.M., and Kappes, J.C. (2002). Emergence of resistant human immunodeficiency virus type 1 in patients receiving fusion inhibitor (T-20) monotherapy. Antimicrob. Agents Chemother. *46*, 1896–1905.

Yoder, A., Yu, D., Dong, L., Iyer, S.R., Xu, X., Kelly, J., Liu, J., Wang, W., Vorster, P.J., Agulto, L., et al. (2008). HIV envelope-CXCR4 signaling activates cofilin to overcome cortical actin restriction in resting CD4 T cells. Cell *134*, 782–792.

Zhu, P., Liu, J., Bess, J., Jr., Chertova, E., Lifson, J.D., Grise, H., Ofek, G.A., Taylor, K.A., and Roux, K.H. (2006). Distribution and three-dimensional structure of AIDS virus envelope spikes. Nature *441*, 847–852.